CHAPTER 3
RESULTS AND DISCUSSION

3.1. Polymer Characterization

3.1.1. Physical Properties

Some physical properties of the thin hydrogel sheets obtained from different synthesis conditions were compared in terms of i) monomer concentrations, ii) crosslinking concentrations, iii) types of crosslinking agent, iv) copolymer of AMPS-Na^+ with NVP and v) copolymer of AMPS-Na^+ with MAA. The polymer or copolymer sheets were hydrated in distilled water at 35.0±1.0°C, as shown in Table 3.1-3.5 respectively.

Table 3.1. Comparing appearance of hydrogels synthesized from AMPS-Na^+ 30-50% w/v using EGDM 1.0% mole as crosslinker.

AMPS-Na^+ concentrations (%w/v)	**Physical properties**
30% w/v	Sticky and weak
40% w/v	Coherent and flexible sheet
50% w/v	Coherent and brittle sheet

.

Table 3.2. Comparing appearance of hydrogels synthesized from AMPS-Na^+ 40% w/v using EGDM and NMBA as crosslinker.

Types of crosslinking	**Physical properties**
NMBA	Coherent and flexible sheet
EGDM	Coherent and flexible more than NMBA

Table 3.3. Comparing appearance of hydrogels synthesized from AMPS-Na^+ 40% w/v using EGDM crosslinker concentrations between 0.1-2.5% mole.

Crosslink concentrations (% mole)	**Physical properties**
0.1% mole	Sticky and weak
0.5% mole	Sticky and weak
1.0% mole	Coherent and flexible sheet
2.0% mole	Coherent sheet and rather brittle
2.5% mole	Coherent sheet and rather brittle

Table 3.4. Comparing appearance of hydrogels synthesized from AMPS-Na^+ 40% w/v with NVP at 25:75, 50:50 and 75:25% wt using EGDM crosslinker 1.0% mole.

AMPS-Na^+:NVP	**Physical properties**
25:75	Sticky and weak
50:50	Coherent and flexible sheet
75:25	Coherent and fragile sheet

Table 3.5. Comparing appearance of hydrogels synthesized from AMPS-Na^+ 40% w/v with MAA at 25:75, 50:50 and 75:25% wt using EGDM crosslinker 1.0% mole.

AMPS-Na^+:MAA	**Physical properties**
25:75	Coherent and flexible sheet
50:50	Coherent and slightly brittle sheet
75:25	Coherent sheet and brittle

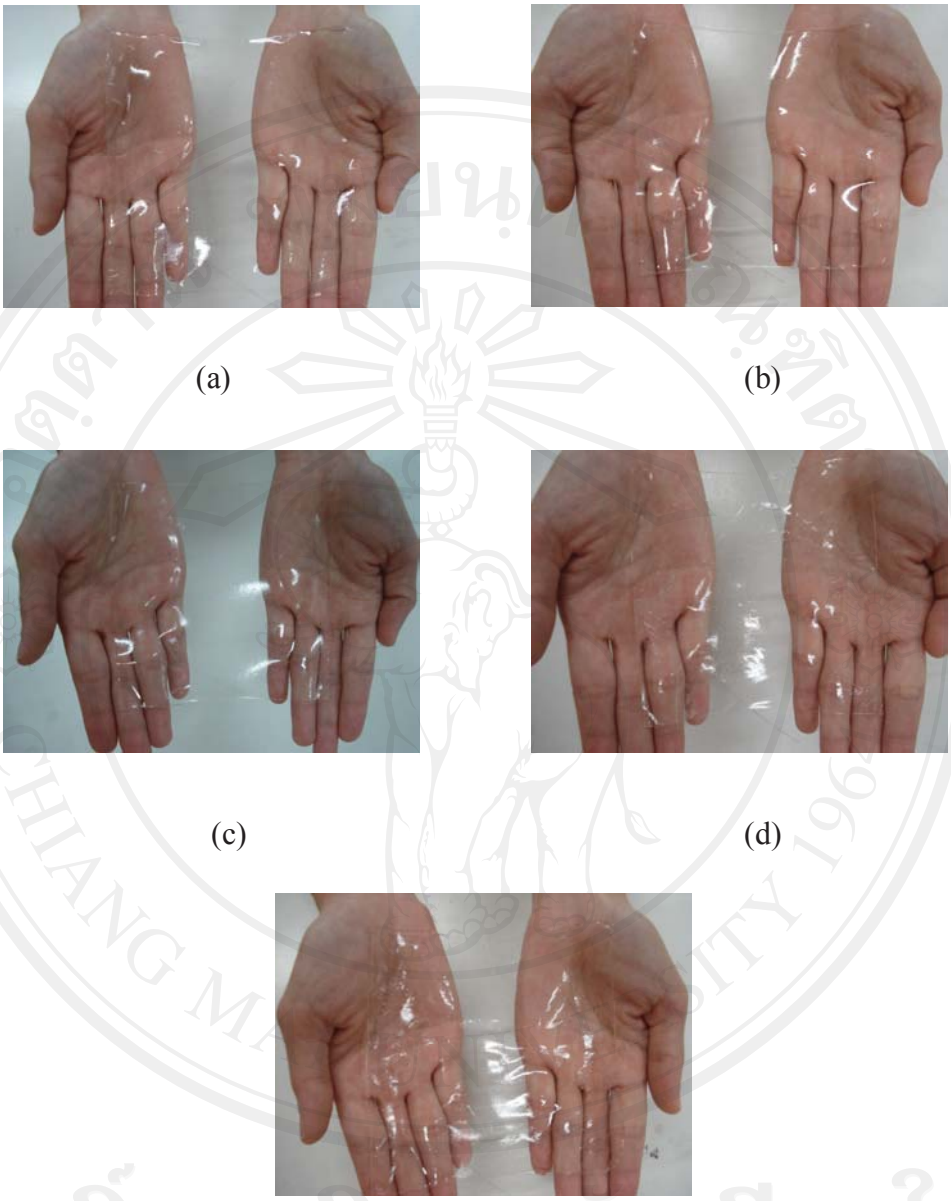

(a) (b)

(c) (d)

(e)

Figure 3.1. The better physical property of hydrogel sheets from Table 3.1-3.5 (a) monomer concentration (40% w/v AMPS-Na^+), (b) type of crosslinking (EGDM), (c) crosslinking concentration (1.0% mole EGDM), (d) 50:50% wt poly(AMPS-Na^+-co-NVP) and (e) 25:75% wt poly(AMPS-Na^+-co-MAA)

All hydrogel sheets were fabricated by method of photoinitiation using UV light and this technique was found to be the most efficient and the most convenient in terms of controlling the polymerization reaction in short period of time. The understanding of the formation mechanism of hydrogels is of great interest in predicting their physical properties. In this work, the sodium salt of 2-acrylamido-2-methylpropane sulfonic acid (AMPS-Na^+) was employed as the main hydrophilic monomer due to its strongly ionizable sulfonate group. AMPS dissociates completely in the overall pH range, and therefore, the hydrogels derived from AMPS exhibit pH independent swelling behavior. It was shown that the linear polymers with sulfonate groups derived from AMPS exhibit extensive expansion in aqueous solutions.

Moreover, the effects of the crosslinker concentration on the physical properties of the polymer were studied. The results show that increasing the crosslinking agent concentration decreases the free volume and the number-average molar mass between crosslinks ($\overline{M}_c$) between the two main backbones. Consequently, the hydrogel sheets became brittle and exhibits low tear strength. It was found that hydrogel sheets prepared from the 1.0% mole EGDM provide better coherency, and superior handing characteristics. In addition, the structure of crosslinking agent (such as EGDM and NMBA) showed a significant effect on the physical properties. The other monomers such as NVP and MAA also received much attention as property modifiers for AMPS-Na^+ due to NVP tends to produce softer hydrogels and slightly tacky with high water content. In case of MAA, it is classic example of pH sensitive carriers that exhibit swelling transitions in response to changes in pH and improve the gel strength property.

3.2. Monomer Characterization

3.2.1. 2-Acrylamido-2-methylpropane sulfonic acid (AMPS)

The Fourier-transform infrared (FT-IR) spectra of the AMPS monomer is shown in Fig. 3.2 compared with the reference spectra in Fig. 3.3. The various peaks in the spectra are assigned to their corresponding bond vibrations in Table 3.6.

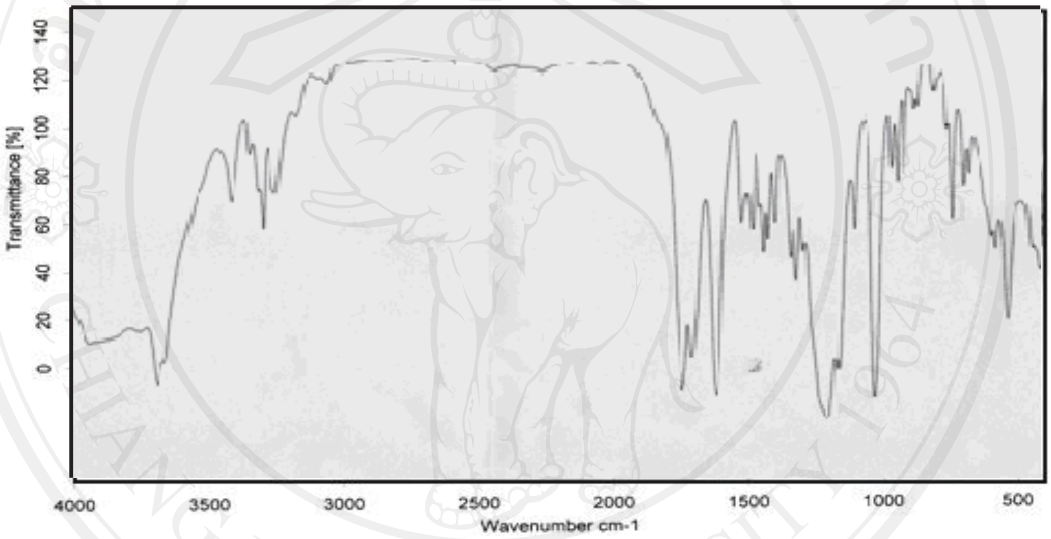

Figure 3.2. Infrared spectra of the AMPS monomer used in this work.

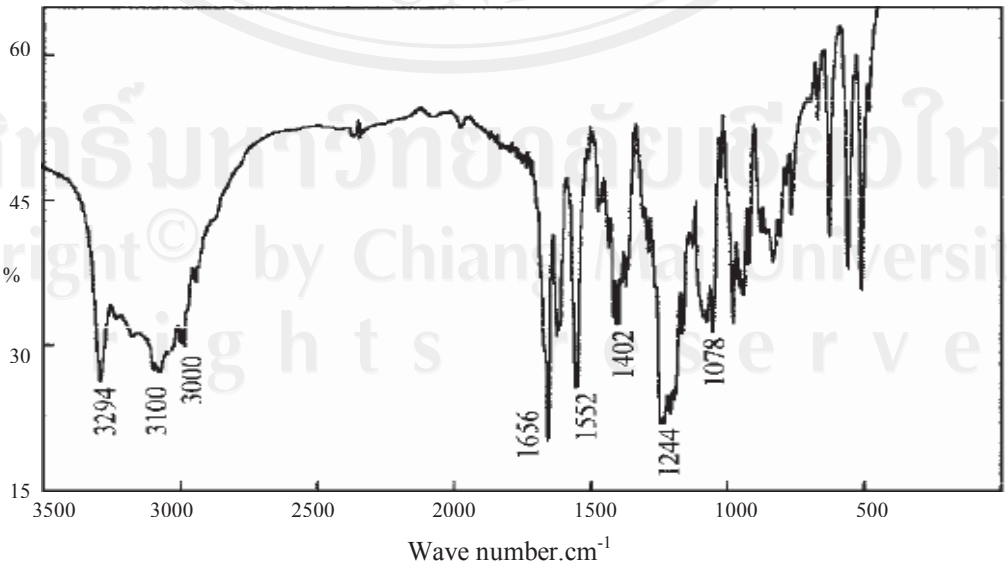

Figure 3.3. Reference infrared spectra of AMPS monomer [121].

Table 3.6. Infrared absorption peak assignments for AMPS monomer.

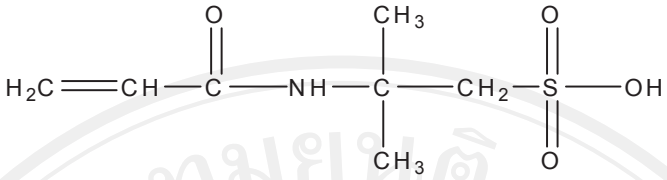

Vibrational Assignment	Functional Group	Wavenumber (cm^{-1})	Peak Intensity*
S=O stretching	$-SO_3$	1373	s
		1245	
C=C bending	CH_2=CH	980	s
C=O stretching	-CONH-	1668	s
N-H stretching	-NH-	~3300	m
		3238	
N-H bending	-NH-	1613	s
C-H stretching	$-CH_2-$, $-CH_3$	~3000-2800	s-m
C-H bending	$-CH_2-$, $-CH_3$	~1450-1375	s, v
S-O stretching	$-SO_3$	650	s
C-N stretching	-C-N-	1127	s
O-H stretching	-O-H	~3400-2800	b

*s = strong, m = medium, v = variable, b = broad

3.2.2. *N*-Vinylpyrrolidone (NVP)

The Fourier-transform infrared (FT-IR) spectra of the NVP monomer is shown in Fig. 3.4 compared with the reference spectra in Fig. 3.5. The various peaks in the spectra are assigned to their corresponding bond vibrations in Table 3.7.

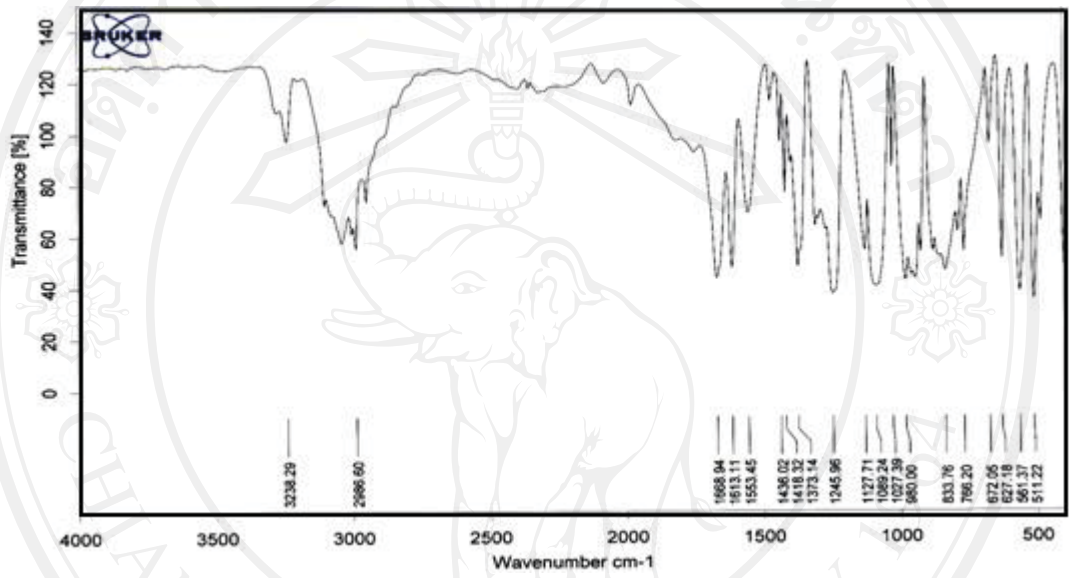

Figure 3.4. Infrared spectra of the NVP monomer used in this work.

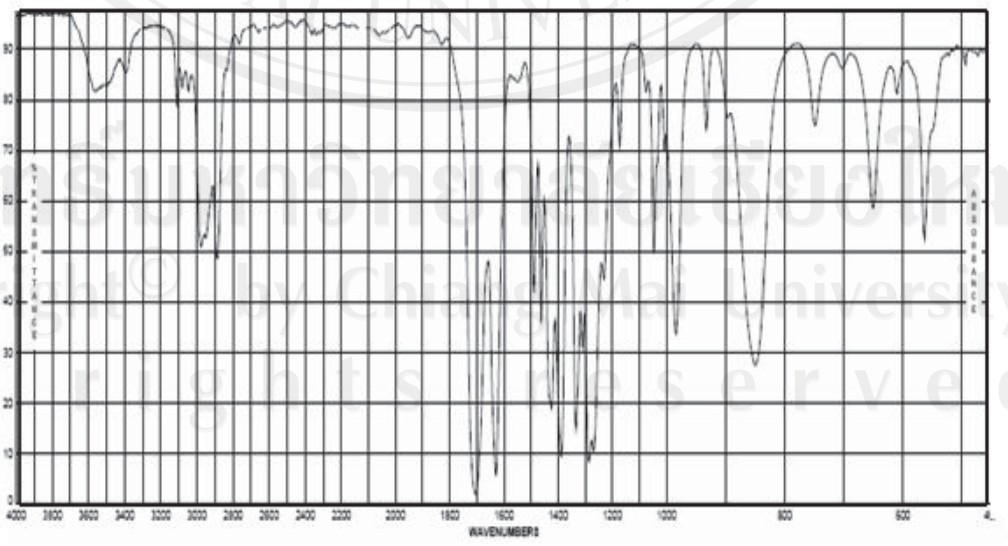

Figure 3.5. Reference infrared spectra of NVP monomer [122].

Table 3.7. Infrared absorption peak assignments for NVP monomer.

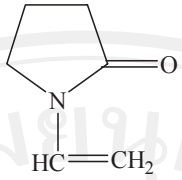

Vibrational Assignment	Functional Group	Wavenumber (cm^{-1})	Peak Intensity*
C=C bending	CH_2=CH	980	s
C=O stretching	-CONH-	1668	s
C-H stretching	$-CH_2-$, $-CH_3$	~3000-2800	s-m
C-H bending	$-CH_2-$, $-CH_3$	~1450-1375	s, v
C-N stretching	-C-N-	1127	s

*s = strong, m = medium, v = variable, b = broad

3.2.3. Methacrylic Acid (MAA)

The Fourier-transform infrared (FT-IR) spectra of the MAA monomer is shown in Fig. 3.6 compared with the reference spectra in Fig. 3.7. The various peaks in the spectra are assigned to their corresponding bond vibrations in Table 3.8.

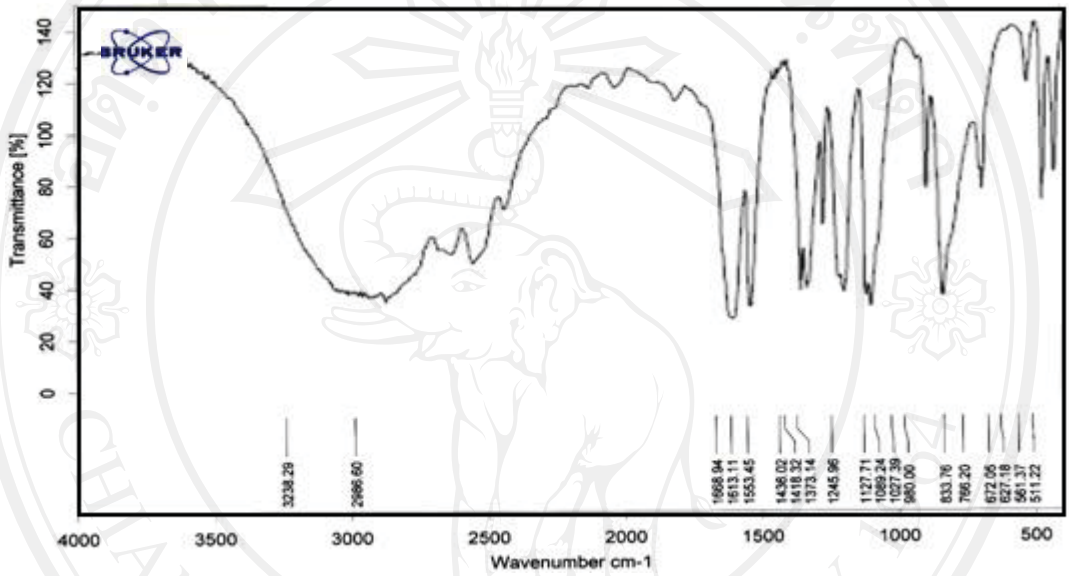

Figure 3.6. Infrared spectra of the MAA monomer used in this work.

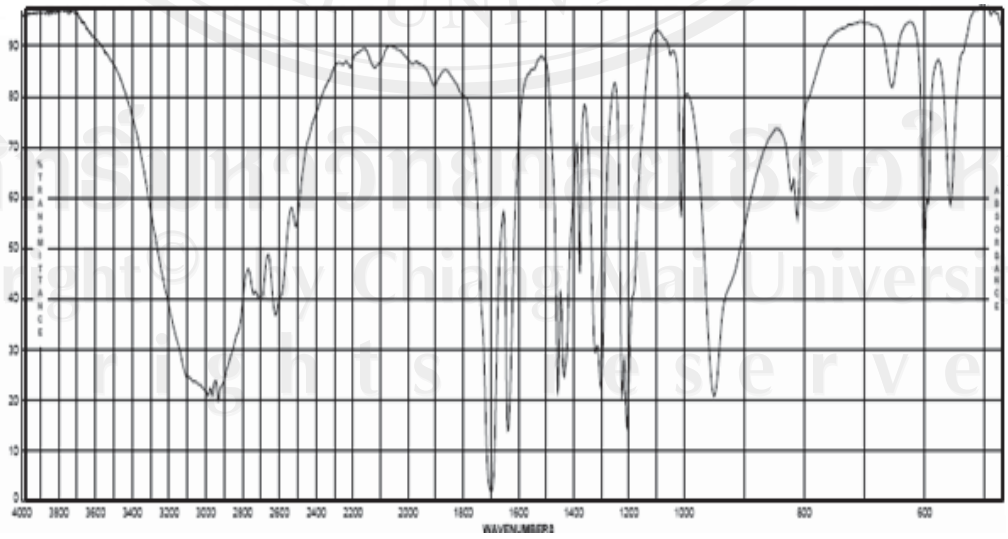

Figure 3.7. Reference infrared spectra of MAA monomer [123].

Table 3.8. Infrared absorption peak assignments for MAA monomer.

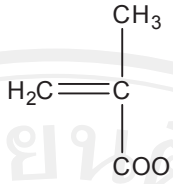

Vibrational Assignment	Functional Group	Wavenumber (cm^{-1})	Peak Intensity*
C=C bending	CH_2=CH	980	s
C=O stretching	-COOH	1700	s
C-H stretching	-CH_2-, -CH_3	2900	s-m
C-H bending	-CH_2-, -CH_3	~1450-1375	s, v
C-O-H stretching	-O-H	~3300-3000	b

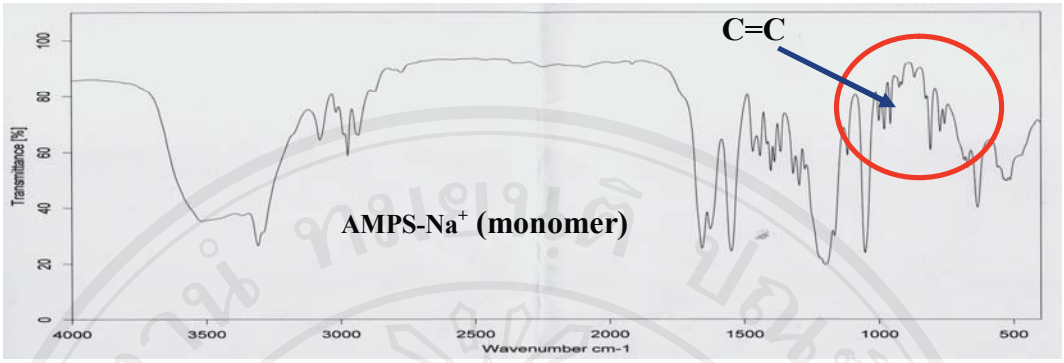

(a)

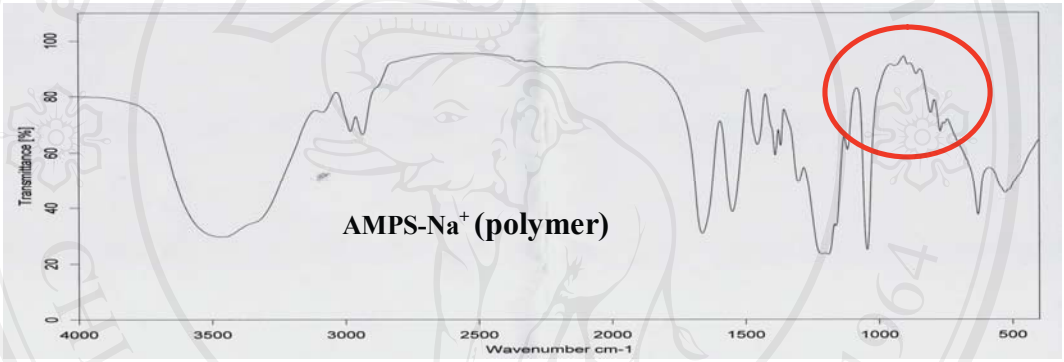

(b)

Figure 3.8. Comparison of FT-IR spectra between (a) AMPS-Na^+ monomer and (b) poly(AMPS-Na^+).

It is indicated in Fig. 3.8 that the signals at 1000-980 cm^{-1}, carbon-carbon double, were disappeared due to the polymerization between monomers occurred through this carbon-carbon double bonds via free radical polymerization. During the reaction, the intensity of these vinyl unsaturation peaks was gradually reduced until approaching a complete conversion. However, it is impossible to identify exactly about the reaction between carbon-carbon double bonds of AMPS-Na^+, NVP or MAA. Therefore, IR spectra are really suitable for their characterization and following up the reaction of hydrogel polymerization by decreasing of the carbon-carbon double bond.

3.3. Determination of Water Content (WC) and Water Retention (WR)

3.3.1. Determination of Water Content (WC)

The water absorption properties were followed by immersing thin hydrogel sheets in distilled water at 35.0±1.0°C. The hydrogels synthesized from each set of conditions were compared in terms of their WC. All synthesized hydrogels from different conditions, such as i) monomer concentrations, ii) crosslinking concentrations, iii) types of crosslinking agent, iv) copolymer of AMPS-Na^+ with NVP, v) copolymer of AMPS-Na^+ with MAA and vi) different of absorbed solutions, were compared from water absorption-time profiles shown in Fig. 3.9-3.14.

The equilibrium water content (EWC) is the most significant single property of the gel since it is the water, held within the polymer substrate, that gives hydrogel their unique properties. Thus, the permeability of the membranes, their mechanical properties, their surface properties, and resultant behavior at biological interfaces are all a direct consequence of the amount and nature of water held in this way. The EWC of hydrogels is governed by a range of factors. These include the nature of the hydrophilic monomer used in preparing the gel, the nature and density of crosslinking agent and external factors such as the temperature and pH of the hydrating medium.

The effect of monomer concentrations on the water content of the hydrogel was studied. Swelling behavior of AMPS-Na^+ hydrogel with varying concentrations of AMPS-Na^+ 30-50% w/v is shown in Fig. 3.9. It is shown that hydrogel sheet synthesized from 30% w/v AMPS-Na^+ absorbed water with a faster rate than 40% and 50% w/v AMPS-Na^+ in first 10 mins and then approach equilibrium. It is noticed that hydrogels with more monomer concentrations could reach to equilibrium level faster than lower ones. Also, it was found that the water content decreased significantly with increasing concentration of AMPS-Na^+ monomers. This can be explained by the fact that increasing monomer concentration in the solution results in a greater number of crosslinked poly(AMPS-Na^+) chains and more compact structure in hydrogel network which decreases swelling.

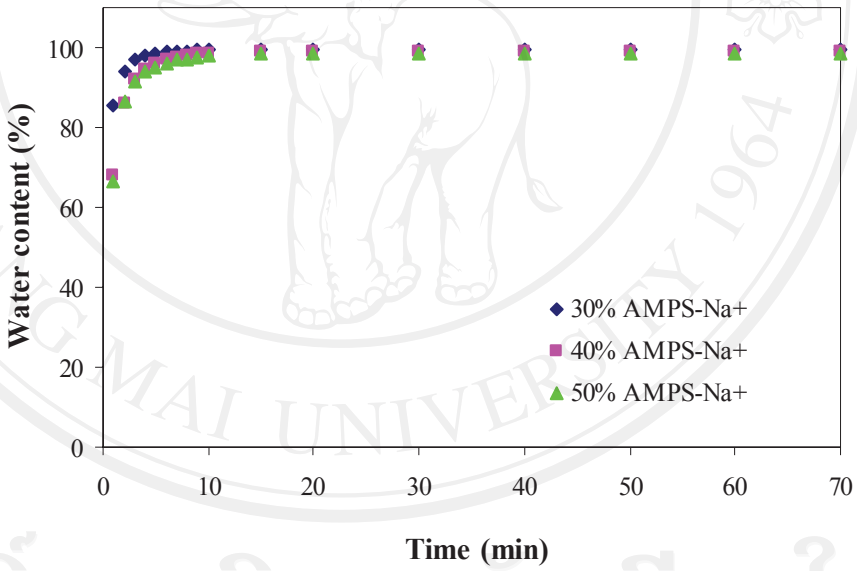

Figure 3.9. Water absorption-time profiles with varying AMPS-Na^+ monomer concentrations from 30-50% w/v using 1.0% mole EGDM crosslinker.

Fig. 3.10 shows the effect of the crosslinker concentrations on the water absorption profiles of the hydrogels, synthesized from 40% w/v AMPS-Na^+ monomer with varying concentrations of the EGDM crosslinking agent. As expected, the water content of the hydrogels decreased with an increasing EGDM concentration because of more crosslink density. Also, the crosslinking density are truely related to the values of the number-average molar mass between crosslinks ($\overline{M}_c$). This can be attributed to the fact that the increasing crosslink density in the hydrogel structure lowers the $\overline{M}_c$ and this curtails the free volume accessible to the penetrant water molecules, thus the swelling ratio decreases. As higher amounts of EGDM were employed, the hydrogel network became less flexible and the equilibrium swelling was attained more quickly. However, at the higher EGDM concentrations of 1.0-2.5% mole, the swelling ratio after 15 mins became constant and the equilibrium level was slightly different from each others. This was probably because the crosslink density of the hydrogel network reached a limit (>1.0% mole), above which the free volume inside the crosslinked network did not vary significantly with further crosslinking.

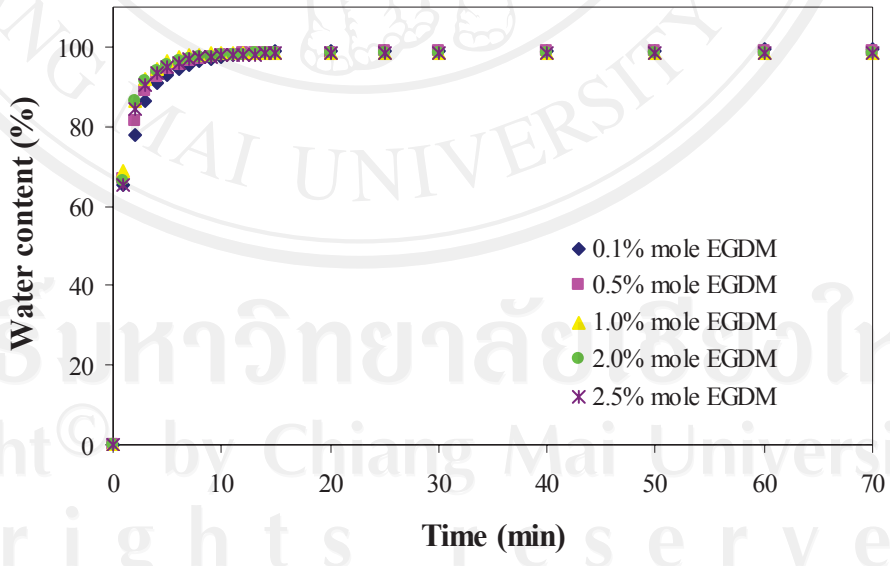

Figure 3.10. Water absorption-time profiles with varying EGDM crosslinker concentrations from 0.1-2.5% mole using 40% w/v AMPS-Na^+ monomer.

The water absorption profiles in Fig. 3.11 reveal that the swelling ratio of the hydrogels, synthesized by EGDM crosslinker, higher than that of NMBA crosslinker, with the same monomer condition. This can be explained by the fact that the molecule of EGDM is longer than that of NMBA, leading to more free volume between polymer chains, which result in less compact structure. Thus, the water molecules could enter to the crosslinked network more easily with a faster rate and reach full absorption at a higher level of absorption.

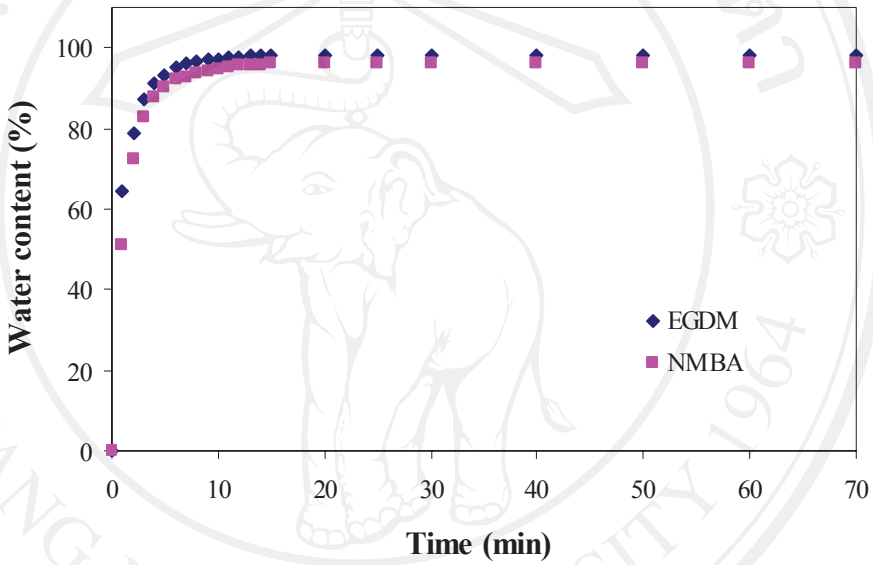

Figure 3.11. Water absorption-time profiles of AMPS-Na^+ 40% w/v hydrogel using 1.0% mole (relative to monomer) with EGDM and NMBA crosslinkers.

Fig. 3.12 and 3.13 illustrate the effect of the copolymers component on the WC. It is clearly shown that WC increased as the percentage of hydrophilic monomer in the copolymer increased. This simply means an incorporation of either NVP or MAA with AMPS-Na^+ offers an easy way of producing homogeneous hydrated copolymer systems which have increased WCs relative to that of only pure AMPS-Na^+ monomer. It was found that at the proportion of 25:75% wt of poly(AMPS-Na^+-co-NVP) and poly(AMPS-Na^+-co-MAA) gave the highest water content because of the copolymers are swollen in water on account of the hydrophilic pendant in their

structure, especially the synthesized copolymer, whose content of NVP and MAA comonomer produced the high water content.

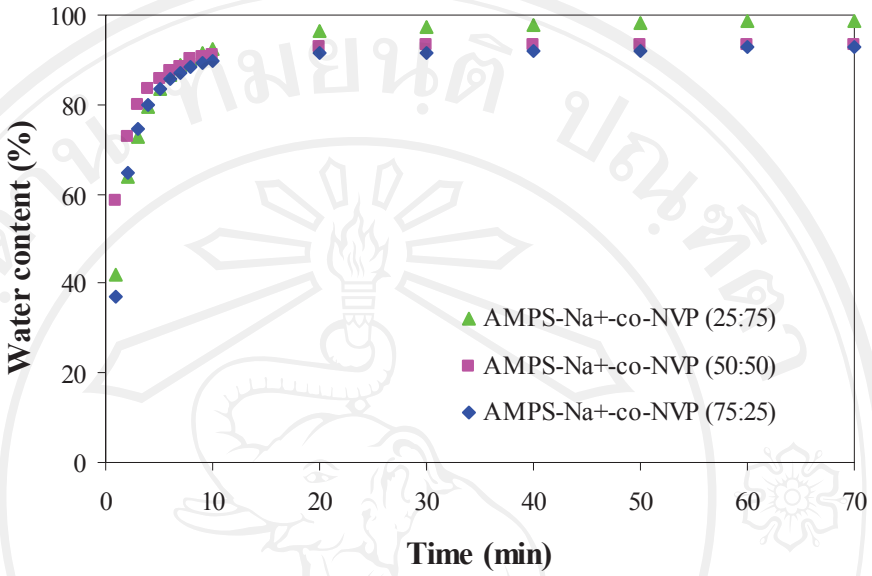

Figure 3.12. Water absorption-time profiles of hydrogel copolymers between 40% w/v AMPS-Na^+ with NVP at 25:75, 50:50 and 75:25% wt using 1.0% mole NMBA crosslinker.

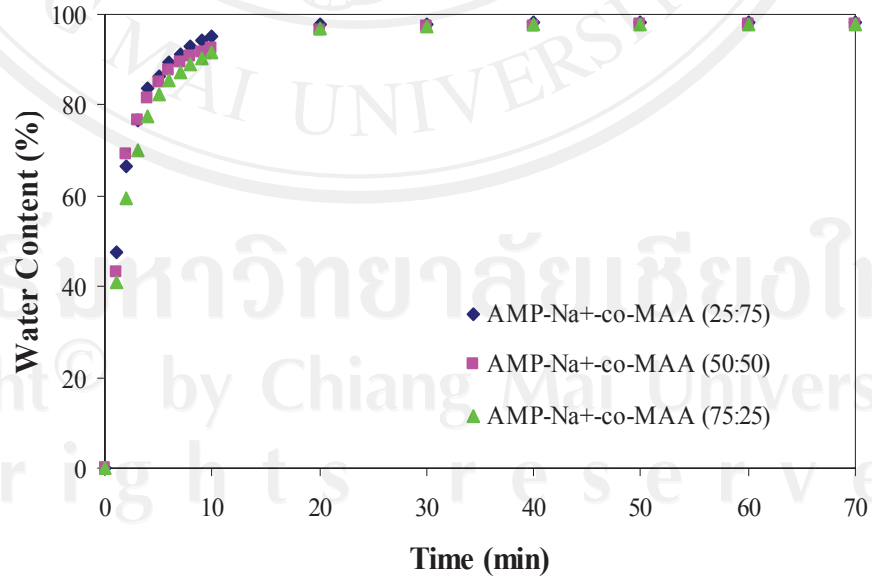

Figure 3.13. Water absorption-time profiles of hydrogel copolymers between AMPS-Na^+ with MAA at 25:75, 50:50 and 75:25% wt using 1.0% mole NMBA crosslinker.

According to Fig 3.14 the ultimate swelling capacities of hydrogels in the synthetic body fluid (SBF) solutions gave the lowest level of absorption as compared with the value which measured in distilled water and saline solution. Generally, swelling values for anionic hydrogels in SBF media are expectedly decreased. This undesired swelling loss has been attributed to the "charge screening effect" of the cations leading to the reduction of osmotic pressure, the driving force for swelling between the gel and the aqueous phases.

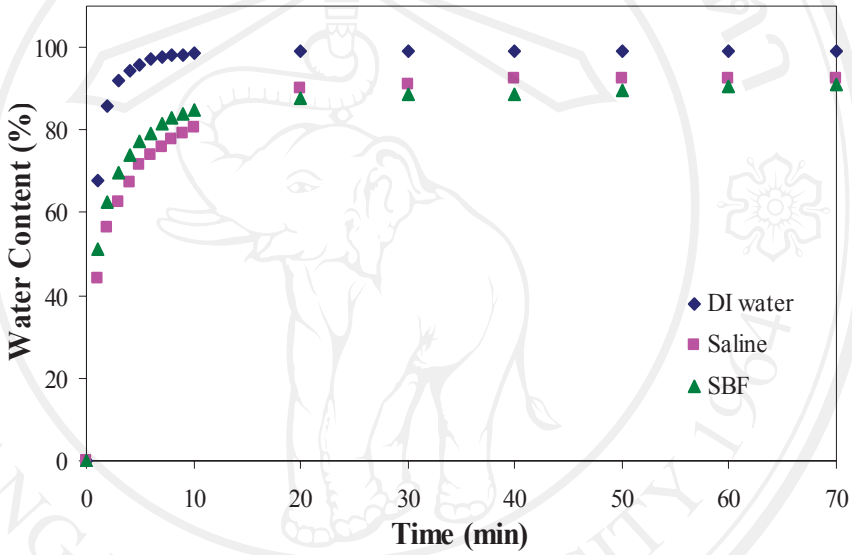

Figure 3.14. Water absorption-time profiles of the AMPS-Na^+ 40% w/v hydrogels prepared from 1.0% mole NMBA crosslinker immersed in distilled water, saline and SBF.

Fig. 3.15 illustrates the effect of cationic charges on swelling ratio. The absorbency of the hydrogel in salt solutions, from high to low is monovalent (Na^+) > divalent (Ca^{2+}) > trivalent (Al^{3+}) cations. It is shown that increasing the charge of the cation resulted in increasing of the degree of crosslinking. Therefore, swelling is consequently decreased due to an increase of electrostatic attraction between anionic sites of polymer chains and multi-valent cations (Ca^{2+} and Al^{3+}) resulting in an increase in the degree of "ion crosslinking".

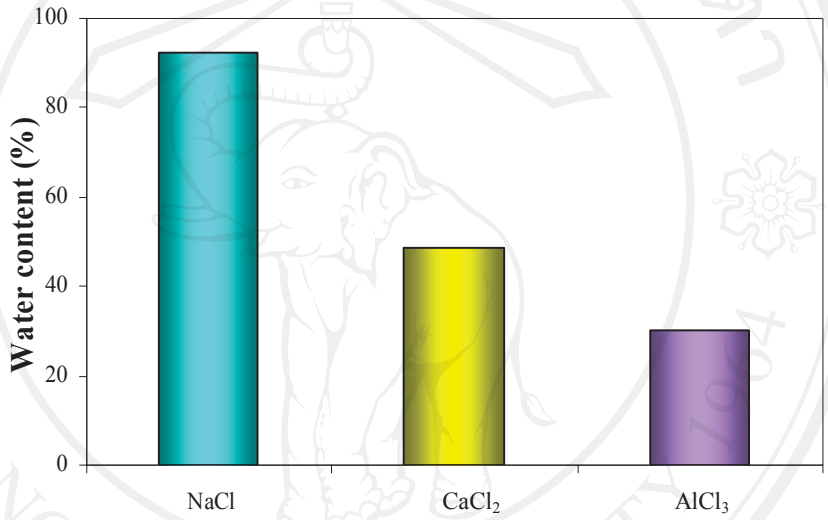

Figure 3.15. Water absorption of the AMPS-Na^+ 40% w/v hydrogels prepared from 1.0% mole EGDM crosslinker immersed in different cationic salt solutions of 0.10 M.

Water absorbency of the hydrogels at various concentrations of salt solutions (0.1, 0.2 and 0.3 M NaCl) decreased with increasing ionic strength of salt solutions, as shown in Fig. 3.16. These results are due to the fact that the osmotic pressure difference between the internal hydrogel network and the external solution is reduced with increasing external solution concentration.

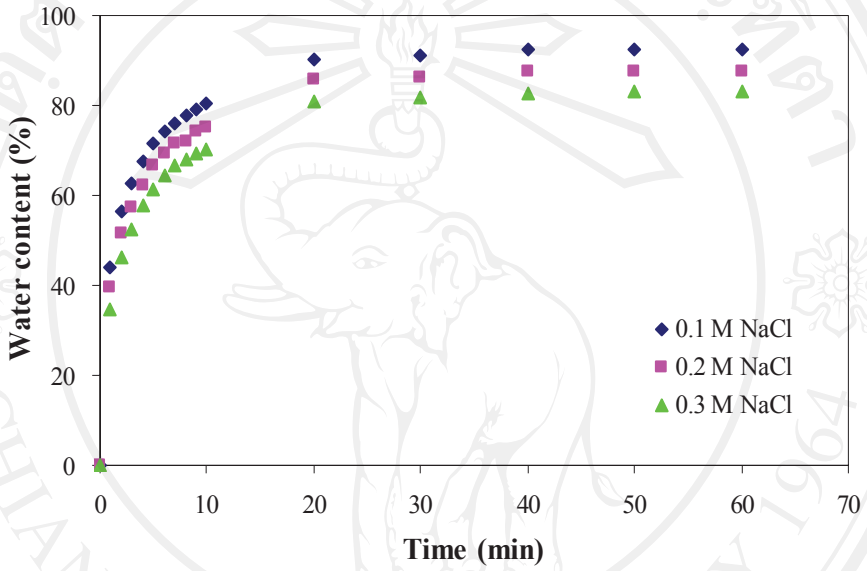

Figure 3.16. Water absorption-time profiles of the AMPS-Na^+ 40% w/v prepared from 1.0% mole EGDM crosslinker immersed in various NaCl concentrations ranging from 0.1-0.3 M.

3.3.2. Water Retention (WR)

The relative rates of water loss of hydrogels synthesized from each set of conditions were compared in terms of i) monomer concentrations, ii) crosslinking concentrations, iii) types of crosslinking agent, iv) copolymer of AMPS-Na^+ with NVP, v) copolymer of AMPS-Na^+ with MAA and vi) difference in absorbed solutions, as shown in Fig. 3.17-3.21.

As a part of characterization, the water retaining capacity of hydrogels was investigated as a function of time. The fully hydrated hydrogels were weighed and the decrease in their weights was measured as a function of time by gravimetry. As expected, the water retention-time profiles in Fig. 3.17-3.21 were the reverse of the absorption-time profile, with rapid evaporative water loss at the beginning followed by a slowing down towards a constant (equilibrium) value. The results showed that the decrease in weight was curvilinear with time.

In Fig. 3.17, the results show that the polymeric gels exhibited water retention behavior decreased significantly with increasing concentration of AMPS-Na^+ monomer. This is because the amide group in AMPS-Na^+ forms an intermolecular hydrogen bond with surrounding water which would turn into an intramolecular hydrogen bond. The state of water molecule in the gel changes from bound water to free water and makes the equilibrium swelling ratio of the gel. The time required for the gels to their equillibrium state increased with decreasing AMPS-Na^+ content in the crosslinked network gel structure.

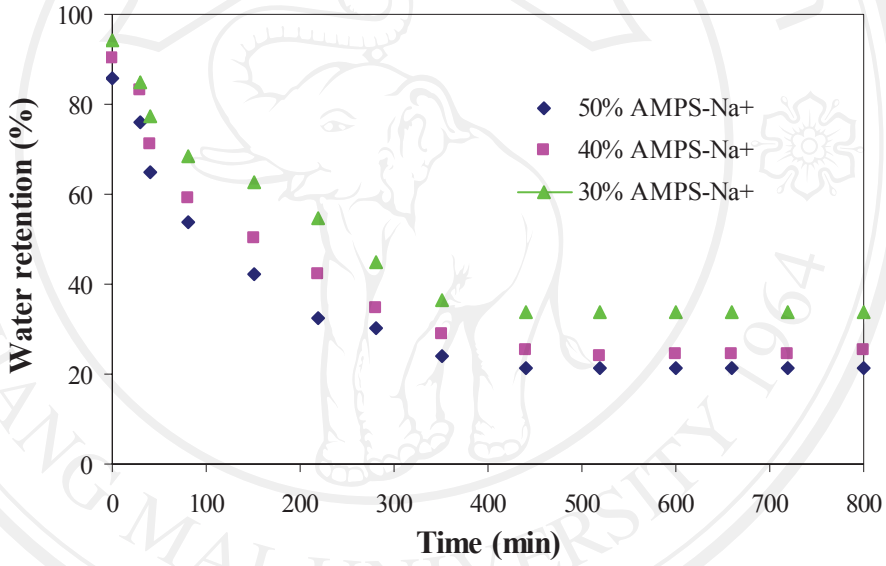

Figure 3.17. Time dependence of the water retentions with varying AMPS-Na^+ monomer concentrations from 30-50% w/v using 1.0% mole EGDM crosslinker.

It was observed in Fig. 3.18 the higher the crosslinking concentration, the more the crosslinking agent was incorporated in the hydrogels structure leading to a tighter and more compact structure. Therefore, crosslinking in hydrogel hinders the mobility of the polymer chain, hence lowering the water retention.

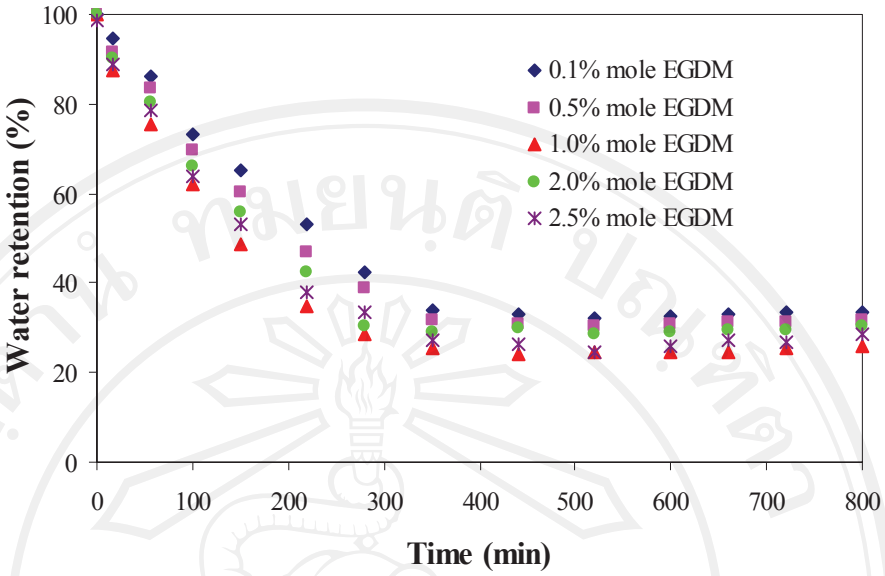

Figure 3.18. Time dependence of the water retentions with varying EGDM crosslinker concentrations from 0.1-2.5% mole using 40% w/v monomer.

The effect of types of crosslinking agent on the water retention was studied. Fig. 3.19 shows that the water retention of hydrogel with EGDM crosslinking agent gave lower level than NMBA crosslinking agent. This is because EGDM has longer molecule than NMBA which probably provide more flexibility to crosslinked network. Also, more space of free volume in the crosslinked polymer could retain more water molecules at the same crosslinker concentration. Although this mechanism must be confirmed after determining the degree of crosslinking, it is informative to note that the water retention value is related to the amount of network space. In addition, a crosslinking agent with longer chain length could provide better crossling network of hydrogel in which a higher water retention would be obtained.

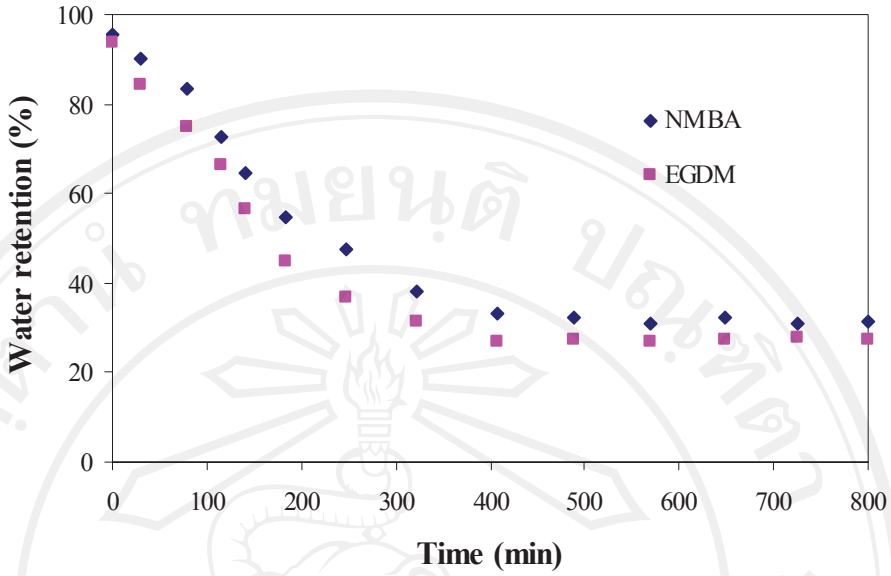

Figure 3.19. Time dependence of the water retentions with different types of crosslinker for hydrogel sheets prepared from 40% w/v AMPS-Na^+ with 1.0% mole crosslinker.

The dynamic water retention of the hydrogel copolymers with different AMPS-Na^+/NVP and AMPS-Na^+/MAA mole ratios are given in Fig. 3.20 and 3.21. The higher level of water retention of hydrogel was found with higher NVP or MAA content which was attributed to the hydrophilicity of NVP and MAA monomers. Incorporation of hydrophilic comonomers could increases the polymer hydrophilicity due to the strong interaction via hydrogen bond between water molecules and the hydrophilic groups in the polymer. Hence, as the hydrophilic monomer was introduced into the polymer chain backbone of the hydrogel, the hydrophilicity of the hydrogel as a whole was improved, leading to an increase in water retention.

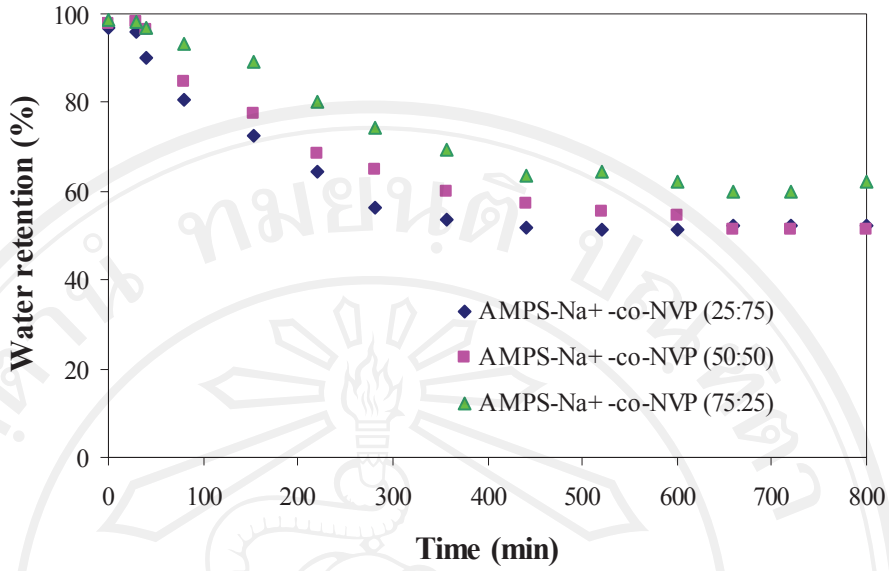

Figure 3.20. Time dependence of the water retentions of AMPS-Na^+ 40% w/v hydrogels with NVP at 25:75, 50:50 and 75:25% wt using 1.0% mole NMBA crosslinker.

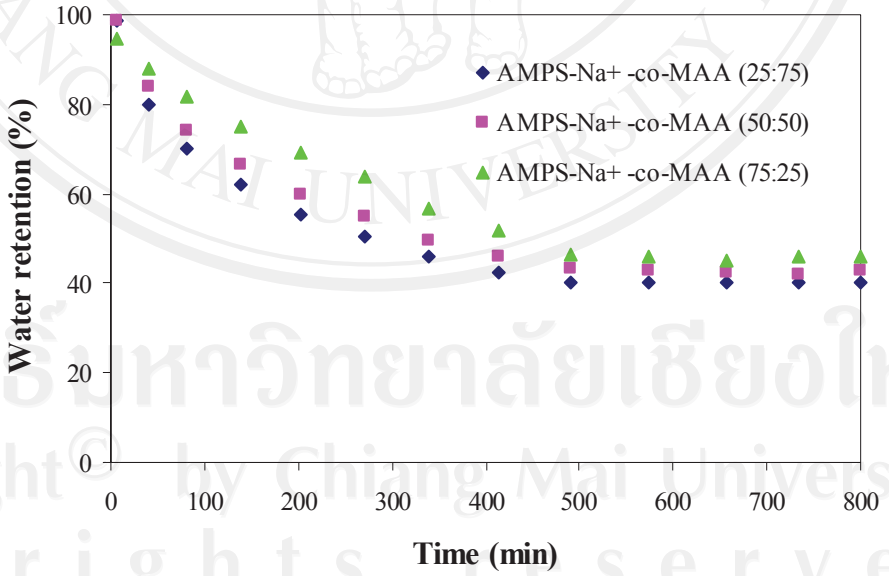

Figure 3.21. Time dependence of the water retentions of AMPS-Na^+ 40% w/v with MAA at 25:75, 50:50 and 75:25% wt using 1.0% mole NMBA crosslinker.

3.4. Water Vapour Transmission Rate (WVTR)

An ideal wound dressing must control the water loss from a wound at an optimal rate. Lamke *et al.* [113], investigated the water vapour transmission across normal and injuried skin. They reported the evaporative water loss for burns, granulating wounds and donor sites along with the average surface temperature. This work has helped the study of burn wound dressings by laying down some guidelines as to the required water vapour transmission of a dressing for a particular injury.

Fig. 3.22 and 3.23 show the loss of water with time from hydrogel sheets at different monomer concentrations and crosslink concentrations of between 30-50% w/v and 0.1-2.5% mole respectively. It was found that the water vapour transmission decreased with increasing monomer and crosslinker concentrations. The hydrogel that comprised of more crosslinked density exhibit rigid structure with less free volume inside the network. Therefore, lower amount of water could retain in this free space. Also, the water molecules are more difficult to diffuse into the structure and this probably lead to an increasing in bound water.

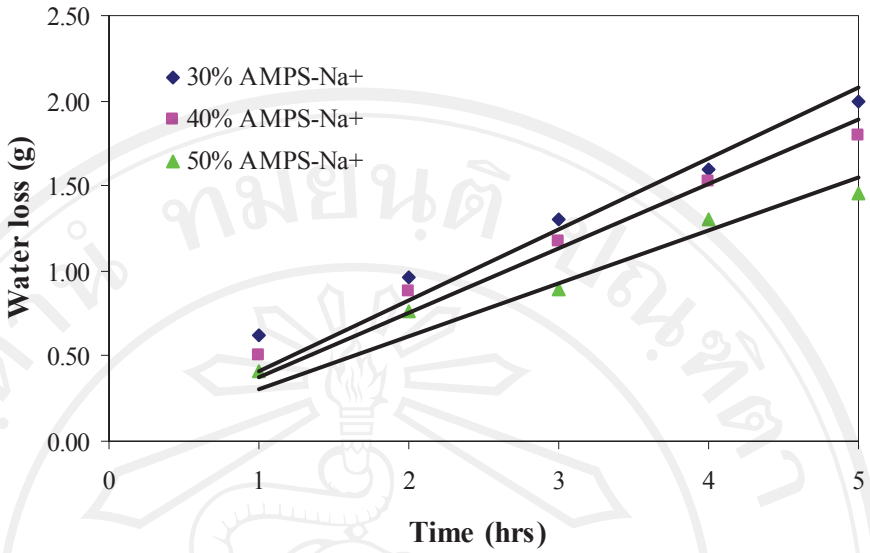

Figure 3.22. Water vapour transmission plot of hydrogel sheets prepared from AMPS-Na^+ monomer at different concentrations.

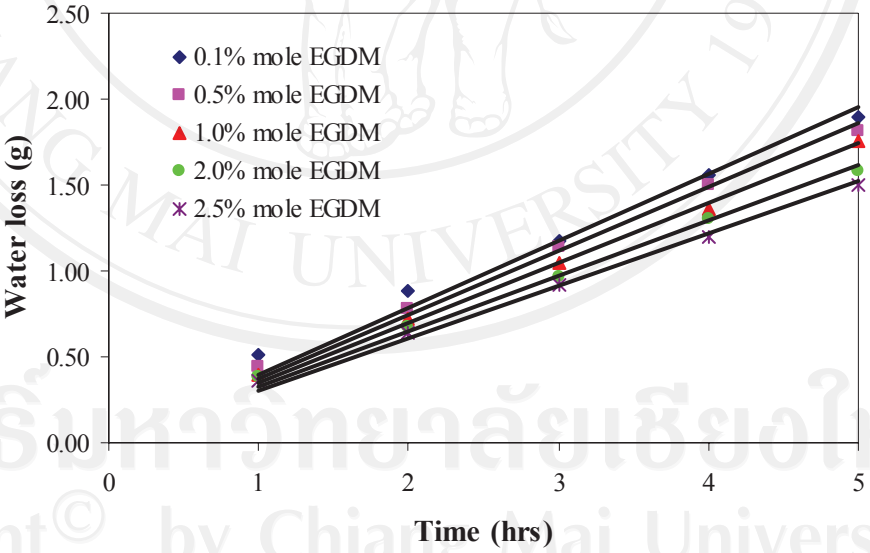

Figure 3.23. Water vapour transmission plot of hydrogel sheets prepared from AMPS-Na^+ 40% w/v at different crosslinker concentrations.

Figure 3.24 shows the loss of water vapour with time using different crosslinkers (EGDM and NMBA). The result showed that EGDM gave higher water vapour transmission than NMBA at the same concentration. This was because hydrogel with EGDM crosslinker created looser crosslinked network which resulted to free more space between polymer chains. Consequently, free water molecules could be filled in and the interaction between these molecules could act as barrier to evaporative water loss.

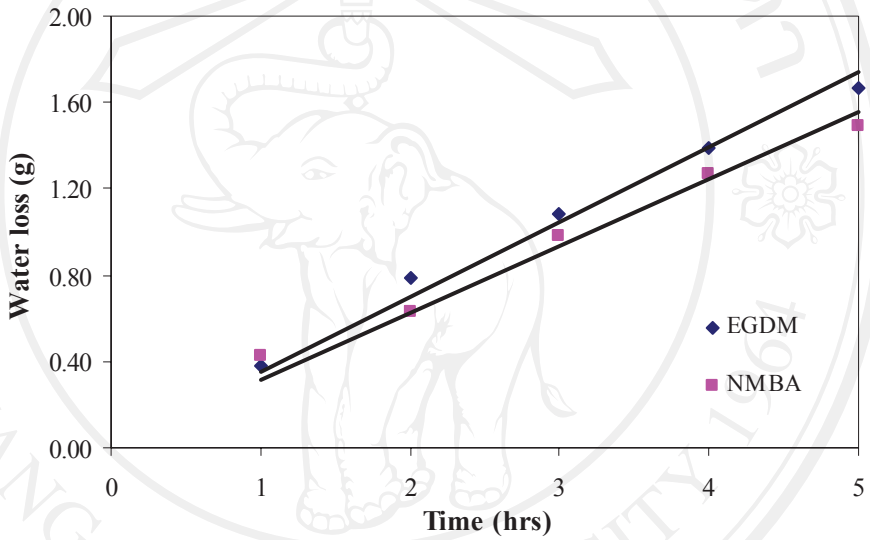

Figure 3.24. Water vapour transmission plot of hydrogel sheets from AMPS-Na^+ 40% w/v with EGDM and NMBA crosslinker.

Fig. 3.25 and 3.26 showed that water vapour transmission increased with increasing NVP and MAA contents in poly(AMPS-Na^+-co-NVP) and poly(AMPS-Na^+-co-MAA). Hydrogels that contained NVP and MAA comprising of the –NH and COO^- groups respectively, which increased hydrophilicity. Therefore, the polar groups from these molecules could induce osmosis of free water molecules into the networks. This term is used to describe networks containing free water that can diffuse through the hydrogel. Thus, poly(AMPS-Na^+-co-NVP) and poly(AMPS-Na^+-co-MAA) seem to provide an effective partial barrier to evaporative water loss.

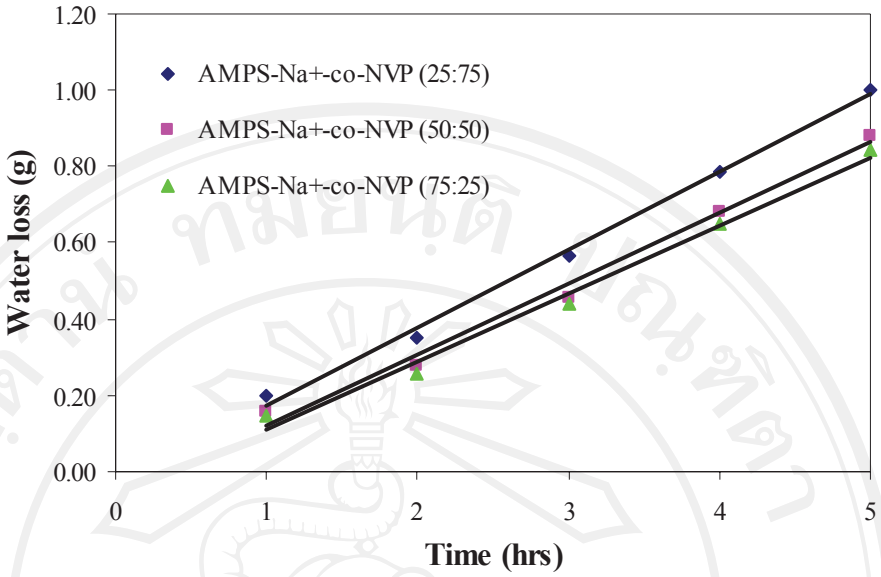

Figure 3.25. Water vapour transmission plot of hydrogel sheets from AMPS-Na^+ 40% w/v with NVP at 25:75, 50:50 and 75:25% wt and 1.0% mole NMBA crosslinker.

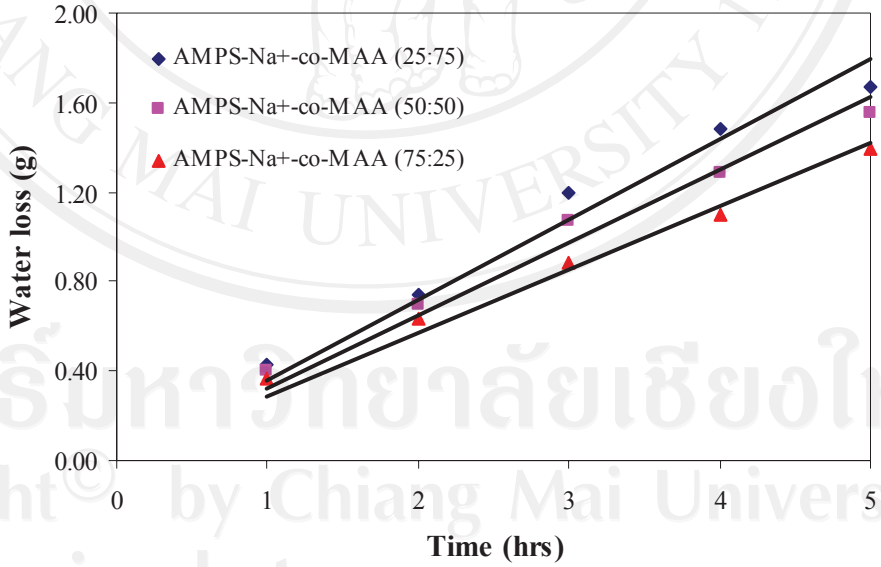

Figure 3.26. Water vapour transmission plot of hydrogel sheets from AMPS-Na^+ 40% w/v with MAA at 25:75, 50:50 and 75:25% wt and 1.0% mole NMBA crosslinker.

From Table 3.9, it is clearly shown that the 2nd degree wound has the highest evaporative water loss. Normally, a covering should have a similar water vapour transmission to that of a skin and allow some exudates remain at wound site to keep wound moist which can accelerate wound healing process.

Table 3.9. The water vapour transmission rate of hydrogel synthesized by various conditions.

Conditions	Polymers	WVTR ($g/hr.m^2$)
	Normal*	8.50
	1st Degree burn*	11.60
	2nd Degree burn*	178.10
	3rd Degree burn*	143.20
Vary %monomer	AMPS-Na^+ 30% w/v	146.75
	AMPS-Na^+ 40% w/v	133.96
	AMPS-Na^+ 50% w/v	109.86
Vary %crosslink	0.1% mole EGDM (AMPS-Na^+ 40% w/v)	138.45
	0.5% mole EGDM (AMPS-Na^+ 40% w/v)	131.52
	1.0% mole EGDM (AMPS-Na^+ 40% w/v)	123.53
	2.0% mole EGDM (AMPS-Na^+ 40% w/v)	113.85
	2.5% mole EGDM (AMPS-Na^+ 40% w/v)	107.28
Vary types of crosslink	1.0% mole EGDM (AMPS-Na^+ 40% w/v)	122.79
	1.0% mole NMBA (AMPS-Na^+ 40% w/v)	110.25
NVP Copolymers	AMPS-Na^+-co-NVP (25:75)	69.05
	AMPS-Na^+-co-NVP (50:50)	59.22
	AMPS-Na^+-co-NVP (75:25)	56.61
MAA Copolymers	AMPS-Na^+-co-MAA (25:75)	127.07
	AMPS-Na^+-co-MAA (50:50)	115.12
	AMPS-Na^+-co-MAA (75:25)	100.35

* [124]

3.5. Diffusion Kinetics

Analysis of the mechanisms of water diffusion into swellable polymeric systems has received a considerable attention in recent years, because of important applications of swellable polymers as biomedical materials. It is well known that the sorption of a solvent in a glassy polymer generally exhibits swelling behavior ranging from Fickian to non-Fickian, particularly when the experimental temperatures are near or below the glass transition temperature of the polymer.

Typically, in a sample of polymer sheet, Fickian sorption dominates when the rate of polymer relaxation is quicker compared to that of solvent diffusion. This is characterized by square-root time dependence in both the amount diffused and the penetrating front position. On the other hand, non-Fickian occurs when the rate of polymer relaxation is slower and rate-limiting. In this case, linear time dependence is observed in both the amount diffused and the penetrating swelling front position. Diffusion in polymers is complex and the diffusion rates should lie between liquids and solids. It depends strongly on the concentration and degree of swelling of polymers.

As mentioned earlier that equation 2.4 was used to determine the type of diffusion of water into the superabsorbent polymer. If $n<0.50$, the diffusion is Fickian, while $0.5 < n < 1.0$ denotes that the diffusion is of a non-Fickian type. Equation 2.4 is applied to the initial step of swelling of about 60%. The plots of ln F vs. ln t in Fig. 3.27, the typical curves of swelling kinetics of the superabsorbent polymers are shown in which n (diffusion exponent) and k (constant characteristics of the polymer network) values could be calculated from the slopes and the intercepts of the straight lines. The values of n and k are presented in Table 3.10. Most of the values of diffusion exponent ranging from 0.15 to 1.0 were determined from different NMBA crosslinker concentrations.

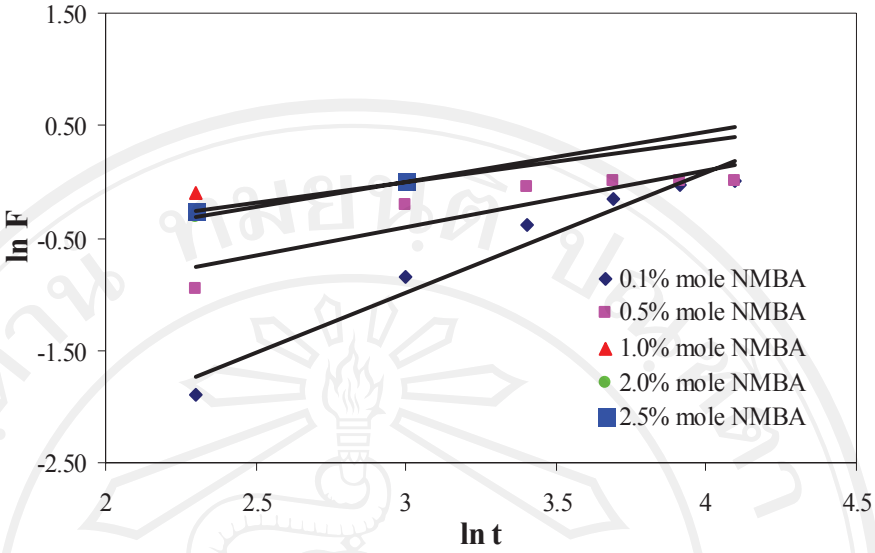

Figure 3.27. Plots of ln F vs ln t (Fickian's diffusion) of the superabsorbent polymers.

As NMBA was used at concentration of 0.1 and 0.5% mole, the diffusion exponent (n) obtained were 0.51 and 1.0 respectively. Hence, diffusion of water into the superabsorbent polymer was taken as a non-Fickian type. The diffusion type was anomalous in behavior, the relaxation time of the polymer matrix and the diffusion time of water were in the same order of magnitude. As a result of slow relaxation, the superabsorbent chains cannot rearrange themselves immediately after the solvent has diffused into the polymer matrix.

Table 3.10. Diffusion exponents (n), diffusion constant (k) and diffusion coefficient (D) of poly(AMPS-Na^+) hydrogel systems in distilled water at 35.0±1.0°C.

Polymers	Concentration of NMBA (% mole)				
AMPS-Na^+ 40% w/v	0.1	0.5	1.0	2.0	2.5
n	1.00	0.51	0.15	0.44	0.37
k x 10^4 (s^{-1})	4.22	1.94	0.46	1.34	1.10
D x 10^9 (cm^2. s^{-1})	3.29	0.76	0.03	0.27	0.09

In case of NMBA crosslinking agent concentrations of 1.0, 2.0 and 2.5% mole, the diffusion exponent (n) were 0.15, 0.44 and 0.37 respectively, leading to the diffusion of water into the polymer matrix corresponding to Fickian diffusion, i.e., the rate of water diffusion was much slower than the expansion of the network. It also implied to the crosslinking effect which corresponded to crosslink density of network.

However, the magnitudes of D values were affected by the concentrations of monomer and crosslinker, which indicated the characteristics of the macromolecular network and penetrant system. For the present work, the D values of hydrogel synthesized from 40% w/v AMPS-Na^+ at varied crosslinking concentration were in the range of 0.03-3.29x10^{-9} $cm^2.s^{-1}$.

3.6. Peel Strength

It clearly shows that hydrogels can be synthesized using various formulations. However, in order to achieve the desired properties, good adhesive and cohesive properties, the ratios of the components need to be altered depending upon the application. Peel strength results yield a relative cohesive strength value of the hydrogel which can be used to assess the integrity of the hydrogel, in conjunction with the strength of the adhesive bond between the hydrogel and the skin on the forearm. The results in Fig. 3.28 and 3.29 shows that all had peel strengths below this value.

Peel strength results from Fig. 3.28 show that reducing AMPS-Na^+ in hydrogel composition decreased the cohesion and adhesion strengths of the hydrogels. Because the strong charge of sulfonate and amide groups of AMPS-Na^+ units in polymer chains were decreased; then intermolecular interaction between chains were decreased. The AMPS-Na^+:NVP (25:75) copolymer hydrogel gave the lowest peel strength. It was less cohesive than the other hydrogels. Then addition of NVP was a useful way of modulating skin adhesion of pure AMPS-Na^+ hydrogel.

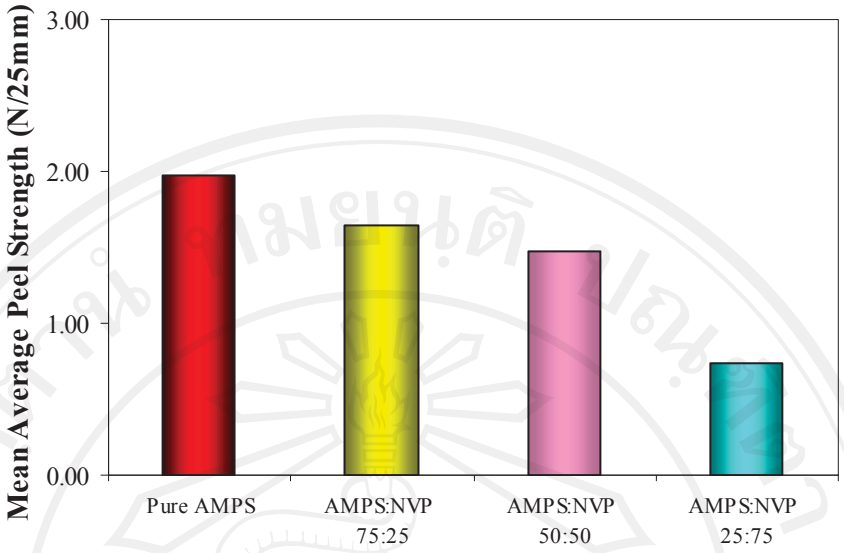

Figure 3.28. A graph showing mean average 90° peel test results for AMPS-Na^+-co-NVP

Peel strength results from Fig. 3.29 show that the cohesive strength of a simple AMPS-Na^+ homopolymer can be increased by the addition of methacrylic acid to each compositions. It was found that addition of methacrylic acid resulted in the increase in the strength of the adhesive bond with considerable improvement in the cohesive properties. By varying the amount of the methacrylic acid, the adhesive and cohesive strength can be controlled, thereby reducing the number of compositions that would need to be investigated. Methacrylic acid has the potential to increase water binding and can remove the interfacial layer of moisture, holding it within the gel. An increase in the quantity of the adhesion enhancer produces higher peel strength hydrogels.

The sodium ion associated with the AMPS-Na^+ has the potential to form the corresponding salt of methacrylic acid, rendering it more water soluble. However, it does not possess a sulfonate group and is less hydrophilic compared to AMPS-Na^+, resulting in a reduction in swelling.

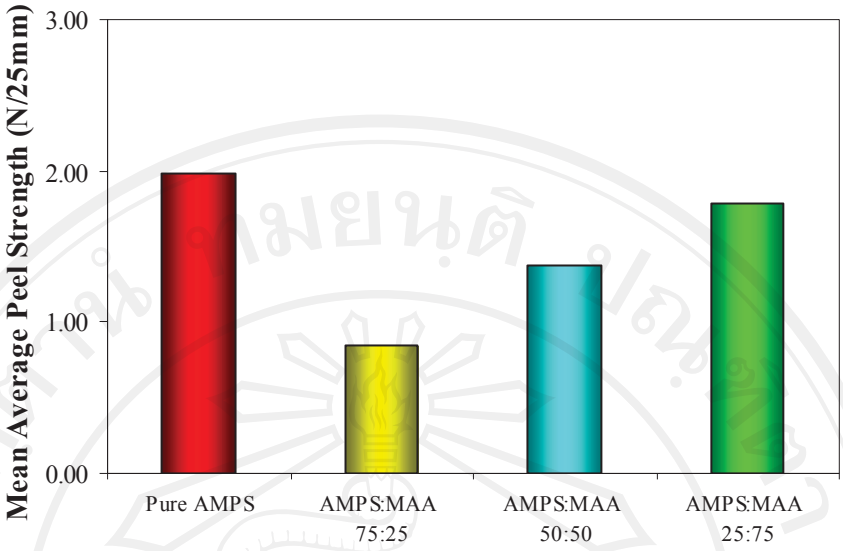

Figure 3.29. A graph showing mean average 90° peel test results for AMPS-Na^+-co-MAA

3.7. pH Dependence of Swelling

A series of pH-sensitive poly(AMPS-Na^+-co-MAA) hydrogels were successfully synthesized by UV-initiated free radical polymerization. This hydrogel is biodegradable and has apparent pH-sensitive character. The effect of pH value on the swelling ratio was determined in buffer media of varying pH, ranging from 1.2 to 9.0, with an ionic strength of 0.1 M at 35.0±1.0°C, as shown in Fig. 3.30. The swelling ratio of hydrogels increased obviously with increasing pH values. It is clearly shows that the content of MAA in the hydrogel network and the pH value of the medium solution have great effect on the swelling ratio of the hydrogel.

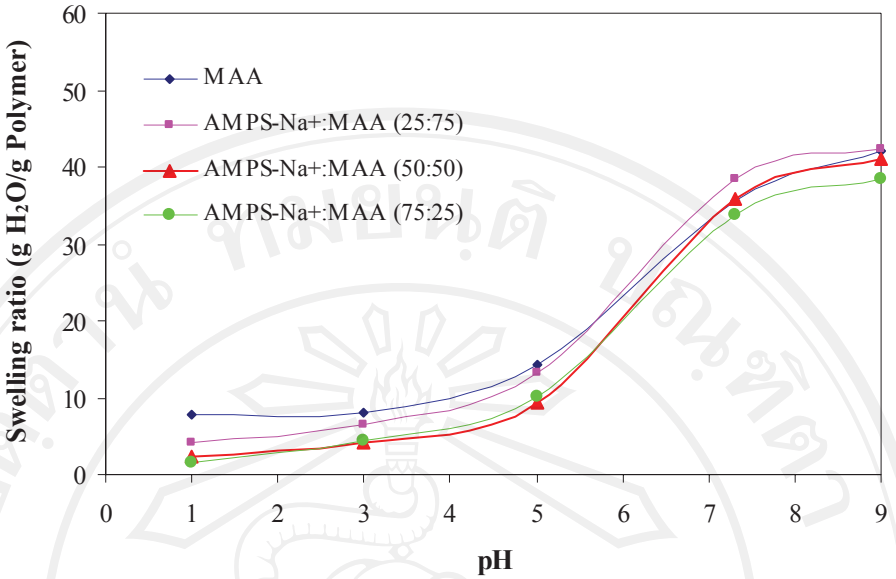

Figure 3.30. The equilibrium swelling ratios of hydrogel in pH ranging from 1.2- 9.0 of buffer solution.

The sensitivity is related to pH-dependent ionization of side carboxylic acid (-COOH) groups of MAA. As the solution becomes acidic (pH = 1.2), most carboxylic acid groups are in the form of COOH, as shown in Fig. 3.31(a). When environmental pH value increased to 7.3, as shown in Fig. 3.31(b), the hydrogen bond broke owing to carboxylic acid groups becoming ionized, resulting in electrostatic repulsions between the ionized groups, which cause swelling degree of the hydrogels to reach to a relatively larger value accordingly. The described biodegradable pH-sensitive hydrogel might have great potential application in biomedical application.

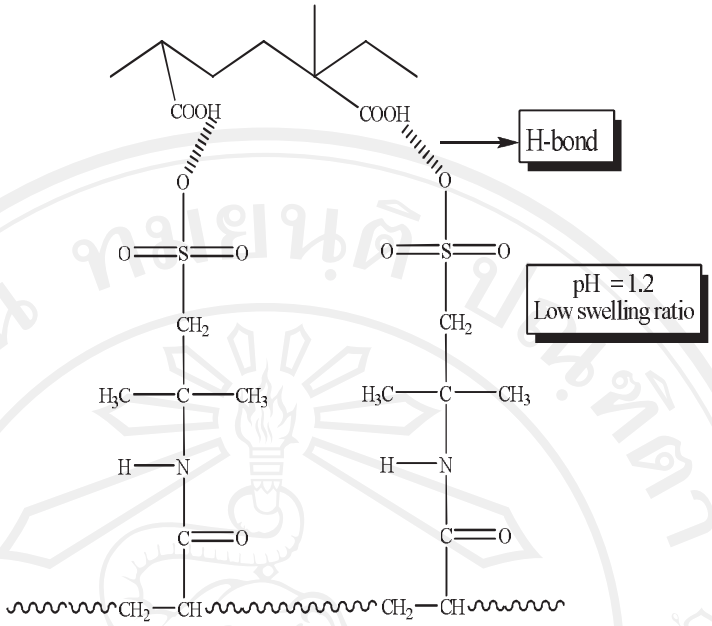

(a)

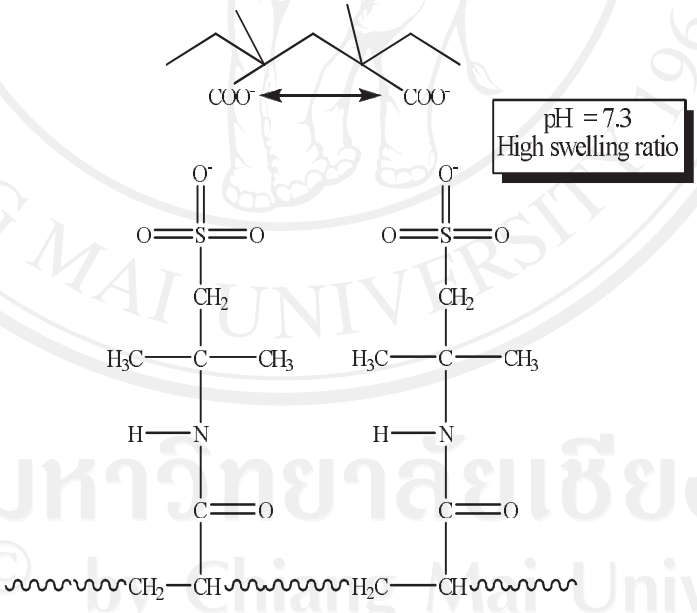

(b)

Figure 3.31. Schematic illustration of the swelling behaviour of pH-sensitive and biodegradable poly(AMPS-Na^+-co-MAA) hydrogel at (a) pH = 1.2 and (b) pH = 7.3 [125].

3.8. Ion Chromatography (IC)

In order to determine the monomers that were least likely to polymerize within the given aqueous-organic environment, the presence and effect of residual monomers had to be established. Having established the monomer most likely to cause the adhesive hydrogel to the relationship of monomer polymerization was explored. The suitability of ion chromatography to quantify the relative amounts of residual monomers was investigated.

The monomer mixture was injected through the column, and the test carried out as described in section 2.12, to determine each monomer′s retention time in order to enable identification of the individual monomer from the residual mixtures. The amount or residual monomer was expressed as a percentage area. By keeping a constant ratio of residual (percentage area) to feed (percentage) of monomer. The chromatogram obtained for AMPS-Na^+ is illustrated in Fig. 3.32.

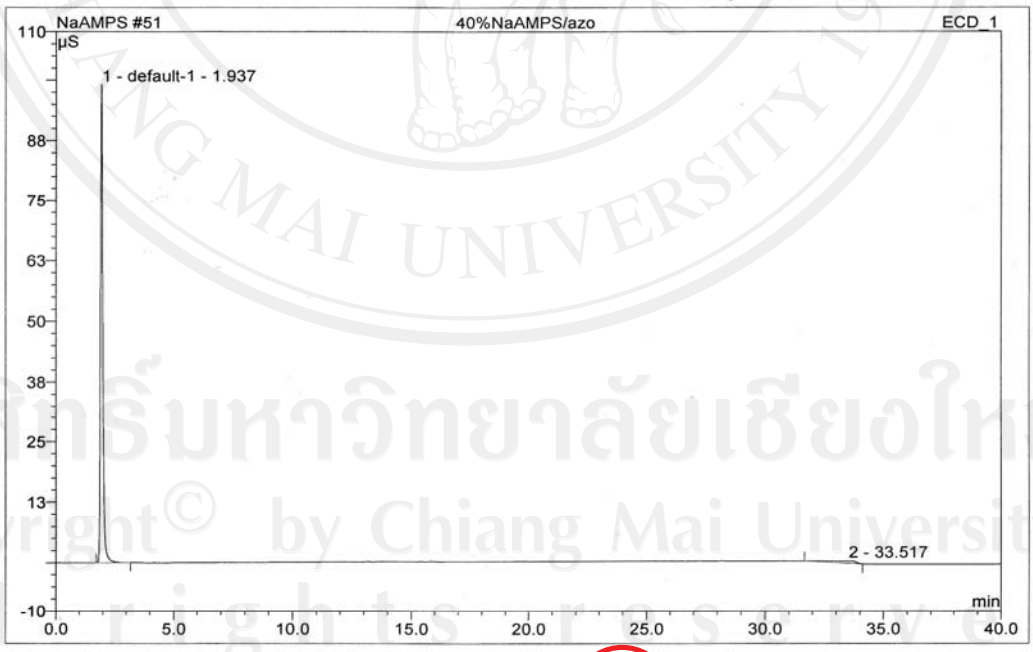

No.	Ret.Time min	Peak Name	Height µS	Area µS*min	Rel.Area %	Amount	Type
1	1.94	default-1	99.103	11.591	95.25	n.a.	BMB
2	33.52	n.a.	0.458	0.578	4.75	n.a.	BMB
Total:			99.562	12.169	100.00	0.000	

Figure 3.32. AMPS-Na^+ ion chromatogram.

The fact that such high levels of residual monomer were obtained indicates that more effective polymerization would be needed before these adhesive hydrogels could be used by humans. This may be achieved by gamma-radiation, which is commonly used by skin contacting medical devices, or simply by more efficient photopolymerization such as those found in commercial photo systems. The use of ion suppression chromatography to identify and quantify anionic monomers was also investigated but met the limited success due to sensitivity issues. Initially there was a steady rise in the baseline suggesting an increase in the signal-to-noise ratio therefore reducing the ability of the software to detect the peaks.

However, it is anticipated that once these are resolved the use of ion suppression chromatography would enable the identification of residual anionic monomers.

3.9. Oxygen Permeability

Oxygen permeability is a vitally important property to consider in the design of hydrogel polymers for use in continuous wound dressings since adequate oxygen is a prime requirement for a healty wound. Hydrogel materials of various water contents which were used for the 'dissolved' oxygen permeability measurements were made in sheet form by copolymerized a hydrophilic monomer (AMPS-Na^+) with others hydrophilic monomer (such as NVP and MAA).

The dissolved oxygen permeabilities of a series of hydrogels having EWC ranging from approximately 20 to 70% were determined at 25^{o}C in an initial series of experiments. The permeabilities, water contents and chemical compositions of the polymers are collected in Table 3.11.

Table 3.11. The water contents and chemical compositions for permeabilities of the hydrogel sheets.

Ratio	%Water content (%WC)			
Copolymers	After synthesized	Partially dehydrated	Fully dehydrated	Fully hydrate
AMPS-Na^+	60	25	0	98
AMPS-Na^+:NVP 75:25	57	24	0	98
AMPS-Na^+:NVP 50:50	55	22	0	93
AMPS-Na^+:NVP 25:75	49	20	0	93
AMPS-Na^+:MAA 75:25	62	23	0	98
AMPS-Na^+:MAA 50:50	59	22	0	98
AMPS-Na^+:MAA 25:75	55	22	0	98

In addition to this, various reported values of oxygen permeability of widely differing specimens. The values thus obtained together with those shown in Table 3.11 were plotted as a function of equilibrium water content (EWC), as shown in Fig. 3.33 and 3.34. It was found that the water content of the hydrogels did not significantly affected D_k because of WCs of the hydrogels were very closely values (80-95%). However, the oxygen permeability is more dependent upon the nature of the comonomers than on the water content of the hydrogel. Even simple structural changes can be used to demonstrate the principle of permeability enhancement in low water content hydrogels.

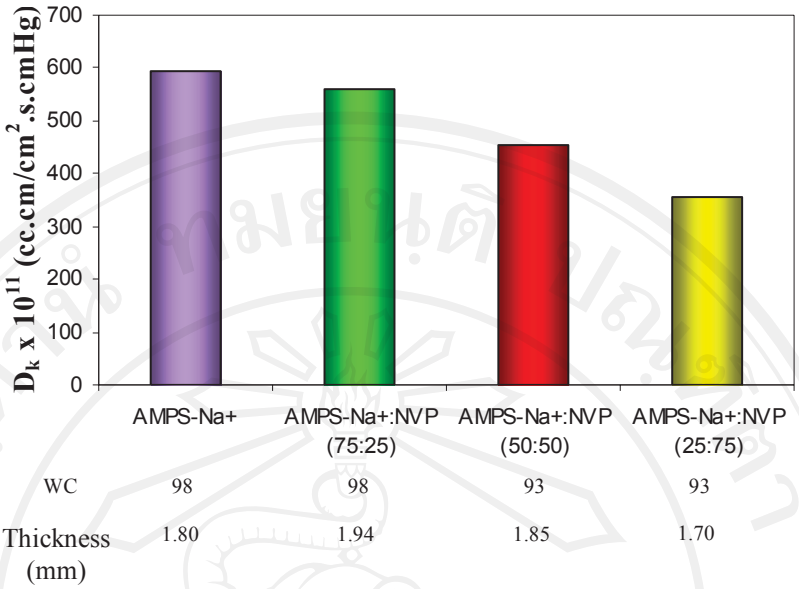

Figure 3.33. Oxygen permeability (D_k) vs thickness (L) and oxygen permeability (D_k) vs water content (%WC) of poly(AMPS-Na^+-co-NVP) hydrogel sheets.

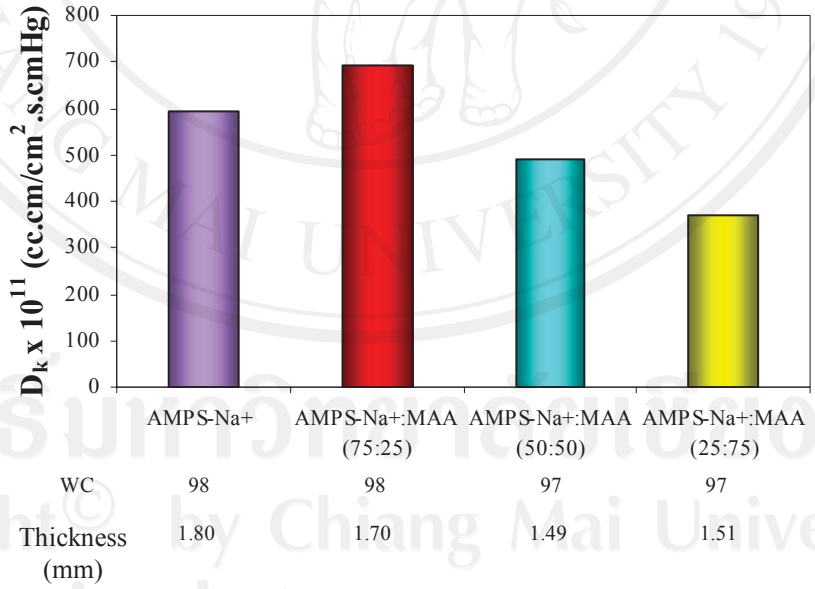

Figure 3.34. Oxygen permeability (D_k) vs thickness (L) and oxygen permeability (D_k) vs water content (%WC) of poly(AMPS-Na^+-co-MAA) hydrogel sheets.

In terms of the design of hydrogel polymers for an applications in which oxygen permeability is important. Since in the work described here it is concerned with increasing the oxygen permeability of hydrogels which are inevitably concerned with relatively high water content materials. Thus, the chemical structure of comonomer has a direct effect for the hydrogel. Further independent experiments confirmed that decreasing of AMPS-Na^+, sulfonate is strong negative charge, can occure hydrogen bond with water molecule was decreased. Due to the water molecule in system decrease. Then, oxygen molecule can diffuse through hydrogel easily more than the system that much water molecule inside, as shown in Fig. 3.35.

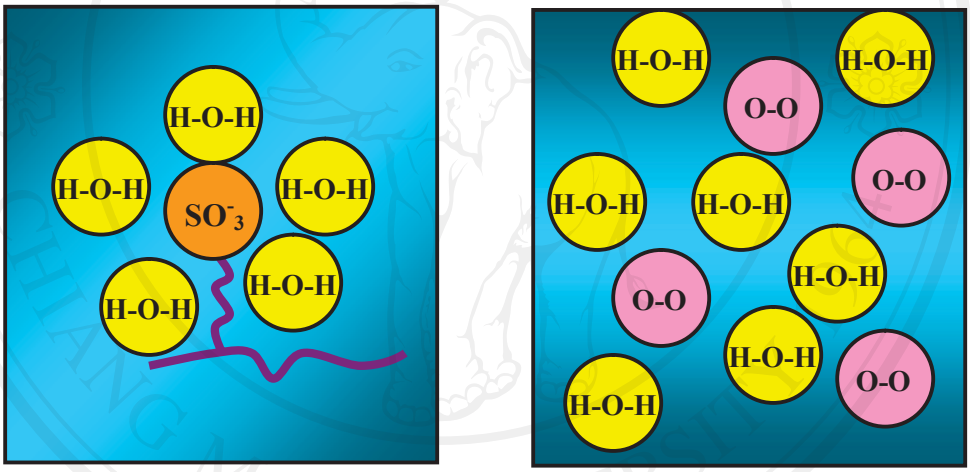

Figure 3.35. (a) Water molecule was interacted with sulfonate anion and (b) Oxygen molecule was barried by water molecule.

In addition, the major problems associated with gels of higher water content are the progressive decrease in strength and increase in linear and volume swell of the material. Both strengths and swell are affected by the chemical structure of the polymer, the major factor in the later (swell) case being the density of the dehydrated polymer. Since the oxygen permeability and linear swell are related to different functions of the water content there will be, for a given class of polymers, a point beyond which increase in water content no longer provides a nett gain in oxygen

permeability. Thus, for a given thickness of dehydrated polymer a point is reached in terms of increasing water content when the increase in linear swell is greater than the increase in oxygen permeability coefficient.

This is illustrated in Fig. 3.36 where the oxygen permeability is divided by the linear swell. Values of the linear swell are those for a terpolymer series in which calculated and measured values agreed to the limit beyond which to experimental results were available (90%). Beyond this point calculated values are used and although there is some difference between linear swell factors of various polymer series these differences are not great. Fig. 3.36 is particularly valuable in that it indicates for a given water content, the oxygen permeability coefficient of the gel expressed per mm of the dehydrate polymer.

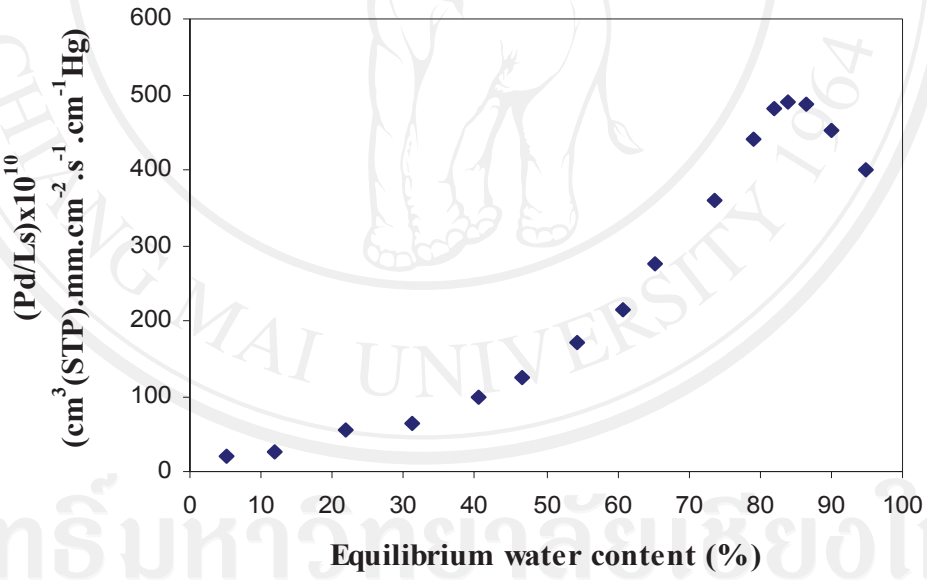

Figure 3.36. Nett increase in 'dissolved' oxygen permeability (Pd) of a series of hydrogels with increasing EWC. The units of Pd are identical to those in the conventional case except that the thickness term (mm) refers to the dehydrated state [126].

3.10. Cytotoxicity

Fig. 3.37 reveals the optical micrographs of the L929 cells in contact with the test specimens. The results clearly demonstrated that poly(AMPS-Na^+), 50:50% wt poly(AMPS-Na^+-co-NVP), and 25:75% wt poly(AMPS-Na^+-co-MAA) were non-cytotoxic. The cells possessed normal morphology after 48 hrs incubation and were well stained with neutral red, indicating that they were alive.

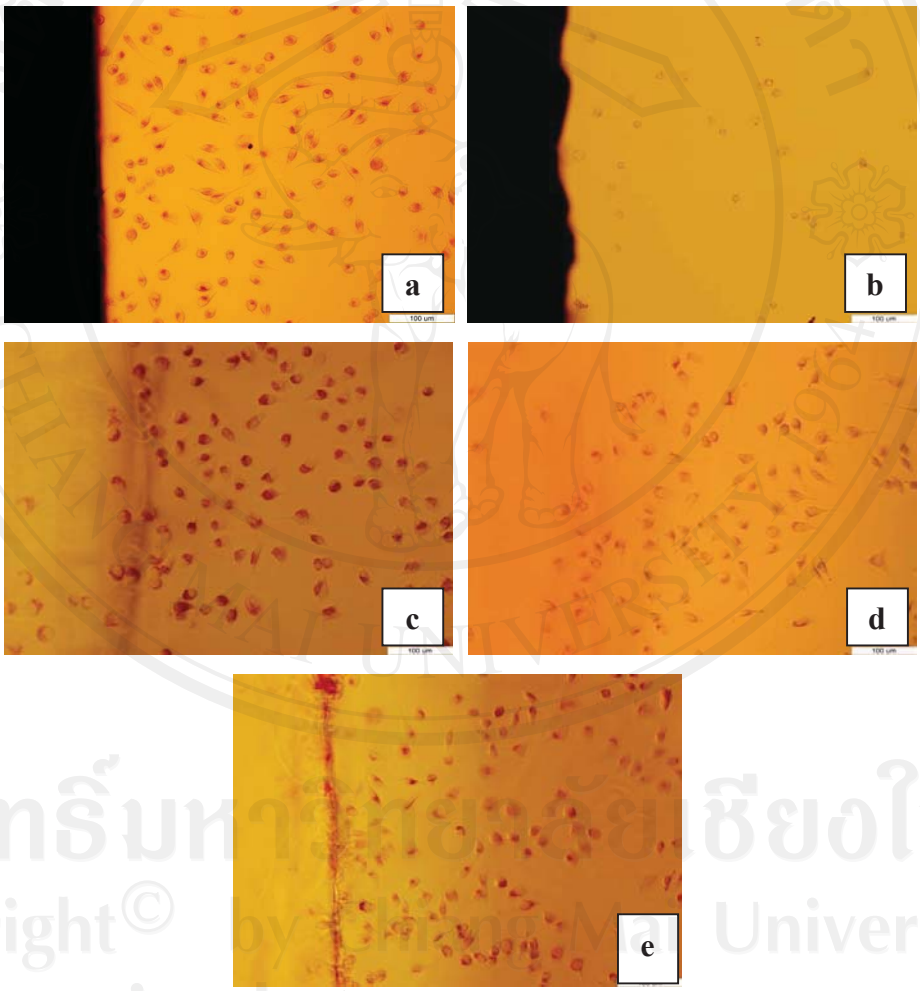

Figure 3.37. Optical micrographs of L929 cells in contact with (A) HDPE (negative control), (B) natural rubber containing carbon black (positive control), (C) poly(AMPS-Na^+), (D) 50:50% wt poly(AMPS-Na^+-co-NVP) and (E) 25:75% wt poly(AMPS-Na^+-co-MAA)